Physics – Uspekhi **52** (8) 835 – 860 (2009)

CONFERENCES AND SYMPOSIA

PACS numbers: 01.10.Fv, **63.20. – e**, 68.35.Rh, **75.80. + q**, **77.55. + f**, **77.80. – e**

Magnetoelectricity
(Scientific session of the Physical Sciences Division of the Russian Academy of Sciences, 20 January 2009)

A A Gorbatsevich, O E Omel'yanovskii, V I Tsebro; A K Zvezdin, A P Pyatakov; A A Mukhin, V Yu Ivanov, V D Travkin, A S Prokhorov, A A Volkov, A V Pimenov, A M Shuvaev, A Loidl; V M Mukhortov, Yu I Golovko, Yu I Yuzyuk

DOI: 10.3367/UFNe.0179.200908g.0887

A scientific session of the Physical Sciences Division of the Russian Academy of Sciences (RAS) devoted to the problem of magnetoelectricity was held on 20 January 2009 in the conference hall of the P N Lebedev Physical Institute, RAS. The following reports were presented at the session:

(1) **Gorbatsevich A A** (St. Petersburg Physico-Technical Center for Research and Education, RAS, St. Petersburg), **Omel'yanovskii O E, Tsebro V I** (P N Lebedev Physical Institute, RAS) "Toroidal ordering in crystals and nanostructures";

(2) **Zvezdin A K** (A M Prokhorov Institute of General Physics, RAS, Moscow), **Pyatakov A P** (A M Prokhorov Institute of General Physics, RAS, Moscow; Physics Department, M V Lomonosov Moscow State University, Moscow) "Inhomogeneous magnetoelectric interaction in multiferroics and related new physical effects";

(3) **Mukhin A A, Ivanov V Yu, Travkin V D, Prokhorov A S, Volkov A A** (A M Prokhorov Institute of General Physics, RAS, Moscow), **Pimenov A V, Shuvaev A M** (University of Wuerzburg, Germany), **Loidl A** (University of Augsburg, Germany) "Terahertz spectroscopy and the magnetoelectric properties of manganite-based multiferroics";

(4) **Mukhortov V M, Golovko Yu I** (Southern Scientific Center, RAS, Rostov-on-Don), **Yuzyuk Yu I** (Physics Department, Southern Federal University, Rostov-on-Don) "Heteroepitaxial films of a bismuth ferrite multiferroic doped with neodymium".

An abridge version of the reports is given below.

PACS number: **77.80. – e**
DOI: 10.3367/UFNe.0179.200908h.0887

Toroidal ordering in crystals and nanostructures

A A Gorbatsevich, O E Omel'yanovskii, V I Tsebro

1. States with a broken symmetry are traditionally the focus of attention of the condensed state physics. The physical nature of a change in macroscopic symmetry is connected with the appearance of this or that type of ordering. The modern technologies of nano- and heterostructures provide the possibility of controlling not only the parameters of the energy spectra and wave functions, but also the macroscopic symmetry of a system. The physical manifestations of the violation of macroscopic symmetry in nanostructures can be more vividly pronounced than in bulk materials [1, 2]. Formally, the response of a system to external actions is determined by a set of matrix elements of the operators of physical quantities, whose structure, in turn, is governed by the macroscopic symmetry of the system. Nanostructures differ from the conventional bulk materials with an analogous symmetry because of the difference in the characteristic spatial scales of the variation of the potential energy determining the symmetry of a system. In bulk materials, this scale is on the level of interatomic distances. In nanostructures, this scale can be substantially larger, reaching the maximum characteristic dimension at which the concept of the wave function of charge carriers remains valid, i.e., the coherence length. Correspondingly, the characteristic scale of spatial changes in the wave functions of charge carriers in the nanostructures is substantially greater than in the bulk materials, and, as a result, the magnitudes of matrix elements determining both the equilibrium characteristics of the system and its response to external actions that disturb equilibrium also substantially exceed those in the bulk materials.

In nonmagnetic materials, the spatial symmetry is determined by the charge distribution. The symmetry of magnetic materials is connected with the ordering of microscopic magnetic moments and currents, which breaks the time-reversal invariance. The type of ordering in this case is characterized by an order parameter [3] whose symmetry corresponds to a change in the macroscopic symmetry of the system upon its transition into an ordered state (in the general case, the order parameter is a tensor which represents one of the irreducible representations of the symmetry group of the low-temperature phase).

Thus, for instance, in the case of a symmetry group formed by the operations of spatial and time inversion, which has four vector representations, four vector order parameters can exist [4, 5]: polar vector of electric polarization **P** invariant relative to the inversion of time t; axial t-odd vector of magnetic moment **M**; polar t-odd vector of the toroid moment **T** whose symmetry also coincides with the symmetry of the electric current **j** and vector potential **A**, and axial t-even vector **G** which characterizes the ordering of spin

Uspekhi Fizicheskikh Nauk **179** (8) 887 – 913 (2004)
DOI: 10.3367/UFNr.0179.200908g.0887
Translated by S N Gorin; edited by A Radzig

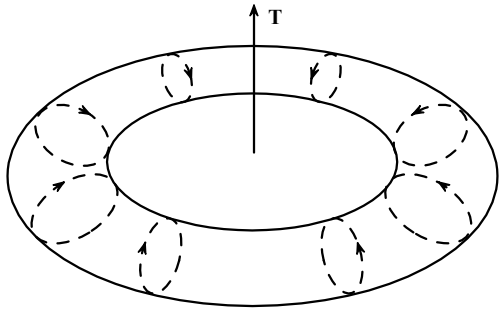

Figure 1. Geometrical image of a toroid moment.

currents in the system. The electric polarization **P** and the magnetization **M** play the role of the order parameters in ferroelectrics and in ferromagnets, respectively.

In the ordered state characterized by a vector **T**, a breakdown of both spatial and time symmetry takes place. This situation is possible in multiferroics — substances in which there coexist ferroelectric and magnetic ordering [6–10]. In multiferroics, the electric effects can substantially change the magnetic properties of the system, and the magnetic field changes the electrical properties, which accounts for the significant interest in these materials from the viewpoint of practical applications. However, the breakdown of both time and spatial symmetry can be connected not only with the presence of magnetic moments and electric polarization, but also with the existence of a nonzero spontaneous electric-current density in systems with toroidal ordering [11].

An object with the symmetry of a toroid moment (Fig. 1) was apparently introduced for the first time by Zel'dovich [12] when considering the phenomenon of parity violation. Parity nonconservation allows the existence of a pseudoscalar a which changes its sign upon coordinate inversion. Consequently, a particle which possesses spin **S** can also be described by a vector **T** related to spin **S** as follows:

$$\mathbf{T} = a\mathbf{S}\,.$$

Later on, a t-odd polar vector in crystals appeared in Ascher's works in connection with the consideration of the possibility of the existence of spontaneous currents [13] and kinetomagnetic and kinetoelectric effects [14], where 31 magnetic classes that allow the existence of this vector were defined. It is important, however, that by itself the electric current **j** cannot be considered as an order parameter, since this is forbidden by the requirement of the gauge invariance of the system energy [15, 16]. Indeed, if it is the current **j** that is chosen as the order parameter, then the Landau expansion for the free energy in a magnetic field H ($\mathbf{H} = \operatorname{rot}\mathbf{A}$), namely

$$F = aj^2 + bj^4 + \ldots - \frac{1}{c}\,\mathbf{jA}\,,$$

is obviously noninvariant relative to the gauge transformation $\mathbf{A} \to \mathbf{A} + \nabla\chi$, where $\chi(\mathbf{r}, t)$ is an arbitrary function.

In the classical theory of electromagnetism, the toroid moments appear as a third independent family (together with electric and magnetic moments) of electromagnetic multipoles [17, 18]. The toroid dipole moment appears in the same order of multipole expansion as the electric and magnetic quadrupoles [17–20]. The connection of the current density with the toroid dipole moment density has the form

$$\mathbf{j} = c\operatorname{rot}\operatorname{rot}\mathbf{T}\,, \tag{1}$$

and the total toroid moment of a volume element is expressed through the current density as follows:

$$\mathbf{T}_\Sigma = \frac{1}{10c}\int \left[\mathbf{r}\,(\mathbf{r}\,\mathbf{j}) - 2r^2\mathbf{j}\right] \mathrm{d}^3 r\,. \tag{2}$$

The role of the conjugate field (source) for the order parameter in the expansion of the free-energy density in the powers of the toroid moment density is played by the total current $\mathbf{J} = (c/4\pi)\operatorname{rot}\mathbf{B}$. In this case, since the symmetry of the toroid moment also coincides with the symmetry of the Poynting vector, the vector product [**EH**] can also serve as its source. Thus, the expansion of the free-energy density in a series in the powers of the toroid parameter in external fields takes the form

$$F = \alpha T^2 + \beta T^4 + \ldots - \gamma\mathbf{T}[\mathbf{EH}] - \mathbf{T}\operatorname{rot}\mathbf{B}\,, \tag{3}$$

where, as usual, $\alpha \propto (\theta - \theta_c)$, θ_c is the transition temperature, and α, β, and γ are the parameters of the material. The concept of the toroid moment as an order parameter was introduced in Refs [5, 11] (see also Refs [2, 21, 22]), and in Refs [23, 24] it was proposed to call substances with a nonzero density of toroid moment toroics.

A toroid moment can be connected with both the orbital currents and localized moments, including those of a purely spin nature. By substituting the expression for the current density written through the magnetization, namely

$$\mathbf{j} = c\operatorname{rot}\mathbf{M}\,,$$

into formula (2), we obtain

$$\mathbf{T}_\Sigma = \frac{1}{2}\int (\mathbf{r}\times\mathbf{M})\,\mathrm{d}^3 r\,,$$

which for the discrete moments goes over into the relationship

$$\mathbf{T}_\Sigma = \frac{1}{2}\sum_i \mathbf{r}_i \times \mathbf{M}_i\,. \tag{4}$$

The simplest configurations of magnetic moments that possess a nonzero toroid moment are displayed in Fig. 2a, b.

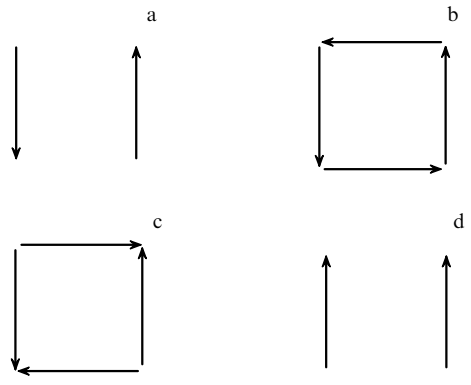

Figure 2. Simplest configurations of magnetic moments: (a, b) with a nonzero toroid moment, and (c, d) with a zero toroid moment (for an explanation, see the main text).

The configuration shown in Fig. 2a also possesses a quadrupole moment, whereas the configuration given in Fig. 2c has a quadrupole moment, but it does not have a toroid moment. Note that, as follows from Eqn (4), the definition of the toroid moment is single-valued and is independent of the choice of the origin under the condition that the total magnetic moment be equal to zero. However, even in the case of a nonzero magnetic moment, for example, in multiferroics, the concept of the toroid moment as an order parameter remains valid [20, 25]. The appearance of a toroid moment at the point of a phase transition in this case can be detected by calculating, according to formula (4), an increase in the toroid moment connected with an increase in magnetic moments. Indeed, for the toroid moment of a system of two magnetic moments M_1 and M_2 (Fig. 2d) oriented along the y-axis and located on the x-axis at the points x_1 and x_2, respectively $(x_2 = x_1 + d)$, we have

$$T_\Sigma = x_1 M_1 + x_2 M_2 = x_1(M_1 + M_2) + dM_2\,, \qquad (5)$$

i.e., the toroid moment obviously depends on the absolute value of x_1, which is connected with the choice of the origin. At $M_1 = M_2 = M_0$, the symmetry of the system does not allow the existence of a toroid moment. This can directly be checked by selecting the origin in the middle between the moments ($x_1 = -d/2$, $T_\Sigma = 0$). The transition into the toroid state occurs upon a change in the magnitudes of the magnetic moments corresponding to the configuration shown in Fig. 2d: $\delta M_{1,2} = \mp\delta M$. The change in the toroid moment, calculated from formula (5), no longer depends on the choice of the origin and coincides with the total toroid moment calculated with formula (5), when the 'correct' choice of the origin in the middle between the moments is made. In experiments, the appearance of a toroid moment can be detected by the appearance of an antisymmetric component of the magnetoelectric tensor $\alpha_{ik} - \alpha_{ki}$. It is precisely in this way that the appearance of a toroid moment was registered at the transition into the spin-flop phase in the strong magnetic field in Cr_2O_3 [26], and in the ferromagnetic compound $Ga_{2-x}Fe_xO_3$ [27]. A toroidal ordering was also revealed in a whole series of other compounds (see Ref. [25]), and recently toroidal domains have been identified by the optical method of the second harmonic generation in the compound $LiCoPO_4$ [28].

The thermodynamic properties of materials with a toroid moment are determined by expansion (3) and are independent of the nature of the toroid moment (spin or orbital), except for the magnitude of the coefficient γ, which characterizes the magnetoelectric effect in the expressions

$$\mathbf{M} = \gamma\,\mathbf{E} \times \mathbf{T}\,, \qquad \mathbf{P} = \gamma\,\mathbf{T} \times \mathbf{H}\,. \qquad (6)$$

In spin toroics, the magnitude of γ is determined by spin–orbit interaction and in the general case this coefficient is small. In the toroics of an orbital nature, this coefficient is determined by the Coulomb interaction and does not contain a spin-orbital smallness; therefore, the magnetoelectric effect can be great.

Figure 3 illustrates the physical mechanism of the appearance of a magnetoelectric effect in an orbital toroic. In the absence of external fields, the magnetic moments of the current contours located symmetrically relative to the toroid axis exactly compensate each other, and the total magnetic moment equals zero. The charge that creates

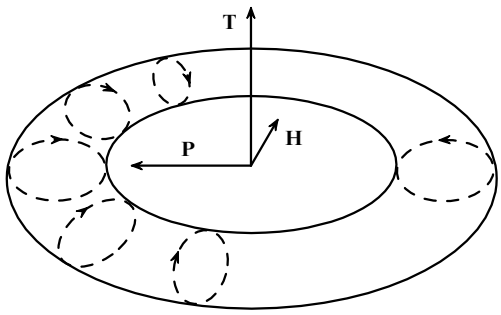

Figure 3. A schematic of the appearance of a magnetoelectric effect in an orbital toroic.

electric currents is also uniformly distributed over the surface of the toroid, and the electric polarization is absent. The external magnetic field orients the local current contours which form the toroid moment. The presence of a macroscopic toroidal symmetry at the microscopic level indicates the existence of a specific hardness of the construction of local currents, which limits their possible deformations. As can be seen from Fig. 3, the current contours are strung on the torus and a change in their orientation is unavoidably connected with a redistribution of the contours over the torus, which is accompanied by a redistribution of the charge and the appearance of electric polarization. On the other hand, the electric field, by transferring the charges, simultaneously moves the current contours over the surface of the toroid, which leads to the disturbance of the mutual compensation of the magnetic moments of elementary current contours and to the appearance of a total magnetic moment of the toroid.

According to formula (6), the toroid moment is dual to the antisymmetric component α_{ik} of the magnetoelectric tensor: $P_i = \alpha_{ik} H_k$, i.e., the toroics represent a subclass of magnetoelectrics [4, 7]. In a wider context, the toroics form a subclass of antiferromagnets. A fundamental difference of the toroics from other antiferromagnets is connected with the fact that the transition into the toroidal state is accompanied by the appearance of a singularity at the transition point of a new response function. This is the function of response to the current:

$$T_{\rm ind} = \chi_{\rm T} J\,, \qquad \chi_{\rm T} \sim \frac{1}{\theta - \theta_{\rm c}}\,,$$

where $\theta_{\rm c}$ is the transition temperature. This function can be measured by placing the specimen between the capacitor plates through which a displacement current is passed, namely

$$\mathbf{J} = \mathbf{J}_D = \frac{1}{4\pi}\frac{\partial \mathbf{D}}{\partial t}\,.$$

The presence of 'its own' conjugated field, whose role is played by the current, as well as of a special response function, explains the need to use, as the order parameter, precisely the density of toroid moment in those antiferromagnets where the symmetry allows its existence.

The special properties of toroics that are orbital in nature manifest themselves at the microscopic level. The presence in the system of a nonzero material t-odd polar vector $\mathbf{T}$, whose symmetry is analogous to the symmetry of the quasimomen-

tum, indicates the possibility of the existence of a linear-in-quasimomentum invariant in the expression for the energy:

$$\Delta E(\mathbf{k}) \propto \mathbf{T}\,\mathbf{k}\,. \tag{7}$$

Thus, the spectrum of elementary excitations in an orbital toroic is asymmetric in the quasimomentum [2, 16]. Depending on the magnitude of the spin–orbit interaction, the asymmetry of the spectrum must also be present in spin toroics, but the asymmetry in this case is small. It should be noted that the orbital antiferromagnetic ordering also appears in models of highly interacting particles [29], where it is known as a 'flux phase'.

The qualitative estimates made in Ref. [11] show that the orbital toroics can possess strong diamagnetism in the nonsuperconducting state (superdiamagnetism). The material magnetization M pertaining to the existence of a current contour with an area S and current J can be represented as $M = aJS$, where a is a certain constant. The paramagnetic component of the response to the external field, δM_S, in this case is related to a change in the area of the contour projection perpendicular to the direction of the magnetic field (i.e., to the orientation of the contour): $\delta M_S = aJ\,\delta S$. The diamagnetic component of the response is determined by a change in the current traversing the contour: $\delta M_J = aS\,\delta J$. When the magnetization serves as the order parameter Δ and the current density $\mathbf{j} = c\,\mathrm{rot}\,\mathbf{M}$, we can write for the total current $J \sim \Delta/\rho$, where ρ is the characteristic dimension of the contour projection ($S \sim \rho^2$). Consequently, $\delta M_J \sim -a\Delta\,\delta\rho$, $\delta M_S \sim 2a\Delta\,\delta\rho$, and the total change in the magnetization $\delta M = \delta M_S + \delta M_J \sim a\Delta\,\delta\rho$ proves to be of the same sign as that of δM_S, i.e., the response of the contour with current has a paramagnetic nature.

If the role of the order parameter is played by the toroid moment density, then the current defined by Eqn (1) is $J \sim \Delta/\rho^2$, and the diamagnetic and paramagnetic components of the response exactly compensate for each other. However, in the case of a spatially inhomogeneous system, there are grounds to expect that the total response will be diamagnetic, since the inhomogeneity can prevent a change in the orientation of the contour with current, thereby suppressing the paramagnetic component of the response.

The microscopic theory of superdiamagnetism [16] in spatially inhomogeneous toroics is based on the analogy between the toroidal order parameter and the vector potential. An essential difference between the toroidal order parameter and the usual vector potential is connected with the fact that the uniform vector potential does not have a physical sense and can be eliminated by a uniform shift in the momentum space (by a gauge transformation), whereas the asymmetry of the spectrum with respect to the quasimomentum in orbital toroics cannot be eliminated by any transformation, and it can lead to the observed physical effects.

In a toroic with a spatially inhomogeneous orbital order parameter, an effective pseudomagnetic field $\mathbf{B}_{\mathrm{eff}} = 4\pi\,\mathrm{rot}\,\mathbf{T}$ can be introduced. The toroidal order parameter in this case plays the role of an effective vector potential. The pseudomagnetic field renders on the charge carriers an action analogous to that of a usual magnetic field. The magnitude of the pseudomagnetic field, which is determined by the nature of toroidal ordering, can be very large in toroics orbital in nature. Correspondingly, the susceptibility χ of the system with respect to the true field B is determined by the differential susceptibility in the total field $B_{\mathrm{tot}} = B_{\mathrm{eff}} + B$:

$$\chi = -\left.\frac{\partial^2 F(B_{\mathrm{tot}})}{\partial B^2}\right|_{B=0}.$$

As is well known [30], the differential susceptibility in strong magnetic fields can be negative and large in magnitude, which is manifested, in particular, in the existence of diamagnetic domains [30, 31]. In the case of a spatially inhomogeneous toroic, the differential susceptibility in a strong pseudomagnetic field is nothing but the response of the system to a weak external magnetic field and, consequently, this response can be strongly diamagnetic.

Pseudomagnetic fields appear also in the description (in the mean-field approximation) of multiparticle effects in models of the quantum Hall effect [32, 33], of superfluid He^3-A [34], and of high-temperature superconductivity with the violation of t invariance [35, 36]. Recently, on the basis of the analogy between the density of the toroid moment and the vector potential, it was shown [37] that in the region of a domain boundary in a multiferroic a pseudomagnetic field appears, which establishes a force that is analogous to the Lorentz force, but acts on light, which explains the mechanism of the optical magnetoelectric effect [38].

The asymmetry of the spectrum in the quasimomentum means that the group velocities of carriers, $V(k) = (1/\hbar)\,\mathrm{d}E(k)/\mathrm{d}k$, with quasimomenta that are equal in magnitude and opposite in direction no longer compensate for each other as in ordinary materials. In this case, the total macroscopic current under equilibrium conditions becomes zero upon integration over the occupied states with the equilibrium distribution function $f_0(k) \equiv f_0(E(k))$, since the integrand is reduced to the total derivative:

$$\mathbf{j} = -2e\int \mathbf{V}(\mathbf{k})\,f(\mathbf{k})\,\frac{\mathrm{d}^3k}{(2\pi)^3} = \frac{2e}{\hbar}\int \frac{\mathrm{d}E(\mathbf{k})}{\mathrm{d}\mathbf{k}}\,f_0\bigl(E(\mathbf{k})\bigr)\,\frac{\mathrm{d}^3k}{(2\pi)^3}$$
$$= \int \frac{\mathrm{d}}{\mathrm{d}\mathbf{k}}\,(\ldots)\,\frac{\mathrm{d}^3k}{(2\pi)^3} \equiv 0\,. \tag{8}$$

However, under nonequilibrium conditions, if the nonequilibrium distribution function is not reduced to a function that depends only on the energy, $f(\mathbf{k}) \neq f(E(\mathbf{k}))$ (i.e., in particular, it does not possess a quasi-Fermi form), the integrand in formula (8) is no longer reduced to the total derivative and in the system there appears a macroscopic current

$$\mathbf{j} = \eta\,\mathbf{T}\,, \tag{9}$$

where η is a dissipative constant. Current (9) constitutes a current flowing in a nonequilibrium system in the absence of a gradient of electrochemical potential. The appearance of such a current is known as the anomalous photogalvanic effect (APGE) [39, 40]. Earlier, APGEs were described in systems without a center of inversion, which were connected with the asymmetry of charge-carrier scattering upon intraband collisions and/or interband transitions [39–42]. The velocity of carriers in this case is an odd function of quasimomentum, and the macroscopic APGE current appears due to an antisymmetric additive to the distribution function in the second order in the variable field. For describing this additive to the distribution function when solving the kinetic equation (or the equation for the density matrix) it is necessary to go beyond the framework of the Born approximation [39].

In bulk materials, states with a nontrivial symmetry are realized, as a rule, as a result of complex interparticle correlations and require the imposition of sufficiently rigorous restrictions on the parameters of interparticle interactions. In nanostructures, a state with an assigned spatial symmetry can be formed using traditional methods of engineering of wave functions, and the violation of invariance with respect to time inversion can be imitated by the action of an external magnetic field. Thus, it has been shown in Ref. [43] that a spectrum asymmetric in momentum, which is characteristic of systems with a toroidal type of ordering, is formed in asymmetric nanostructures (tunnel-coupled asymmetric quantum wells) in a magnetic field **H** parallel to the layers. The presence in this system of a material vector **T** with a symmetry of the toroid moment, which determines the asymmetry of the spectrum with respect to the quasimomentum, directly follows from symmetry considerations:

$$\mathbf{T} \propto \mathbf{l} \times \mathbf{H}, \tag{10}$$

where **l** is the polar vector directed along the axis of growth of quantum wells.

As to the electric polarization

$$\mathbf{P} \propto \mathbf{T} \times \mathbf{H} \tag{11}$$

in the magnetoelectric effect (MEE), it follows from formulas (10) and (11) that two types of MEEs nonlinear in the magnetic field should exist, namely, so-called longitudinal and transverse magnetoelectric effects. In the case of the longitudinal (with respect to the growth direction, i.e., to the asymmetry vector **l**) effect, the electric polarization changes in weak magnetic fields quadratically in the field strength:

$$P_x = \alpha_{\parallel} H_z^2, \tag{12}$$

where $\mathbf{l} \parallel x$, and $\alpha_{\parallel}$ is a proportionality factor depending on the degree of departure from equilibrium. Notice that, because of the symmetry of the system and the presence in it of a polar axis **l**, there is a certain polarization $\mathbf{P}_0 \propto \mathbf{l}$ even in the absence of external fields. The longitudinal magnetoelectric effect represents an addition to $\mathbf{P}_0$ related to the deformation of the wave functions of charge carriers in the magnetic field.

Of greater interest is the transverse magnetoelectric effect, in which case the plane of a heterostructure is inclined relative to the direction of the magnetic field in such a manner that one component of the magnetic field, H_z (which forms the toroid moment), is directed along the plane of quantum wells, and another, H_x (which causes a redistribution of current orbits in the toroidal configuration), is oriented along the asymmetry vector **l** of the heterostructure. In this case, an electric polarization arises in the lateral direction of the heterostructure along the plane of the quantum wells:

$$P_z = \alpha_{\perp} H_z H_x \propto H^2 \sin\varphi \cos\varphi \tag{13}$$

(here, φ is the inclination of the plane of the heterostructure relative to the direction of the magnetic field, and $\alpha_{\perp}$ is the corresponding proportionality factor), which occurs already on a scale of the lateral dimensions of the heterostructure, which in practice corresponds to dimensions on the order of several millimeters (but can also correspond to substantially greater sizes). Therefore, the transverse MEE, in contrast to the longitudinal effect, can easily be observed, and the preparation of specimens in this case does not require the application of lithography to creating the potential contacts, because it suffices to have two alloyed metallic contacts of arbitrary size and shape, spaced apart on the plane.

In the case where the breakdown of the symmetry relative to time inversion is caused by an external magnetic field, it is of interest to study the nonequilibrium properties, for the observation of which it is fundamentally important that the spectrum of elementary excitations be asymmetric.

2. The photogalvanic effect (PGE) and the magnetoelectric effect (MEE) were measured by our team both on undoped asymmetric heterostructures, in which no equilibrium charge carriers exist, and on doped structures with a finite density of equilibrium carriers. In both cases, we always used the photoexcitation of nonequilibrium carriers from the valence band by illuminating the heterostructure with light consisting of photons with the energies greater than the energy gap width (band–band transitions). In the case of PGE, the strength of the spontaneous current, according to formula (9), is determined by the degree of departure from equilibrium of the entire electron system and in doped structures with a significant number density of equilibrium carriers proves to be substantially less (as experiments showed, by many orders of magnitude) than in undoped structures.

As to the MEE, its appearance is primordially in no way caused by the nonequilibrium behavior of charge carriers and is a consequence, as was said above, of a redistribution of current trajectories of the orbital motion of charge carriers, which are responsible for the toroid moment, simultaneously with which there occurs a redistribution of the charge itself in the transverse or longitudinal (with respect to the asymmetry vector) direction. However, in this case as well, as was noted in Ref. [43], the magnitude of the electric polarization is very sensitive to the degree of departure from the system equilibrium, since the expression for the electric dipole moment in the first approximation contains the total derivative of energy with respect to the quasimomentum and vanishes when summing over occupied states with an equilibrium distribution function. According to paper [43], with switching-on dissipation, for instance, by using optical excitation, we should expect a sharp increase in electric polarization. As to the equilibrium polarization, it, in the limit of a strong magnetic field, should arise only in higher orders of magnitude in the holding potential [43].

It should be noted, however, that it is impossible to observe equilibrium polarization in a system with free equilibrium carriers, i.e., in a metallic system, such as a doped heterostructure, since under equilibrium conditions the electric field inside a metallic system should be zero. In our case this means that the redistribution of charge carriers caused by factors that are responsible for the magnetoelectric effect is completely compensated by free carriers in such a manner that a uniform charge distribution would be established over the entire volume. Thus, it occurs that, for doped (metallic) asymmetric heterostructures as well, the observation of a magnetoelectric effect is possible only under nonequilibrium conditions, i.e., in our case, upon optical excitation of charge carriers.

Samples of asymmetric heterostructures investigated, the scheme of measurements, and the geometry of experiments on the photogalvanic and magnetoelectric effects. Experiments on

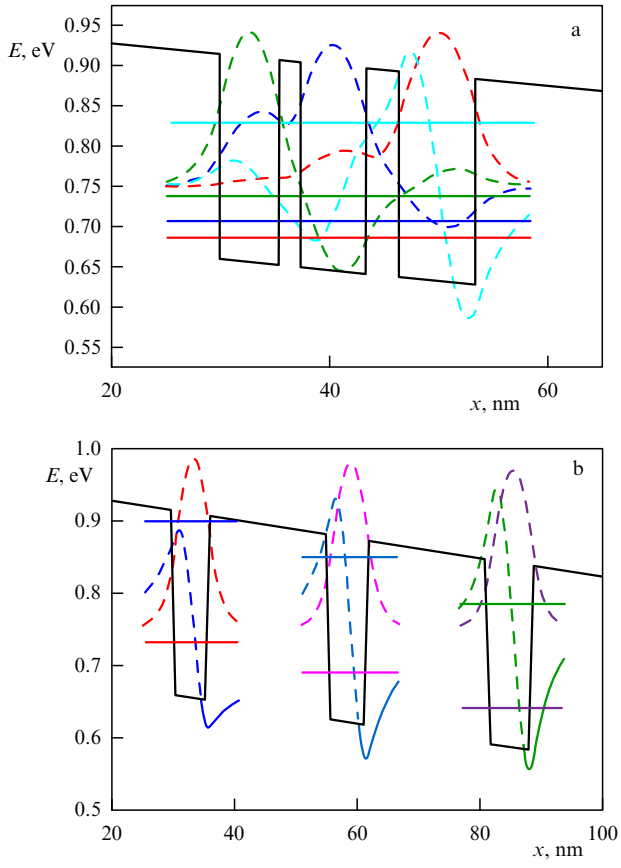

Figure 4. Energy profiles of two asymmetric undoped three-well $Al_xGa_{1-x}As/GaAs$ ($x = 0.25$) heterostructures with (a) tunnel-coupled (S1) and (b) separated (S1a) quantum wells. Levels of the size quantization and corresponding electron wave functions are shown.

Table 1. Layer-by-layer arrangement of two asymmetric undoped three-well $Al_xGa_{1-x}As/GaAs$ ($x = 0.25$) heterostructures with tunnel-coupled (S1) and separated (S1a) quantum wells.

Layer composition	Layer thickness, Å		Comment
	S1	S1a	
GaAs	100	100	Protective layer
$Al_xGa_{1-x}As$	200	200	
GaAs	54	54	Quantum well
$Al_xGa_{1-x}As$	20	200	Barrier
GaAs	60	60	Quantum well
$Al_xGa_{1-x}As$	30	200	Barrier
GaAs	70	70	Quantum well
$Al_xGa_{1-x}As$	200	200	
GaAs	5000	5000	Buffer layer

the observation of photogalvanic and magnetoelectric effects were performed on asymmetric (with respect to the growth direction) heterostructures of GaAs/AlGaAs and AlGaAs/InGaAs/GaAs systems grown by the molecular beam epitaxy (MBE) method. The following samples were investigated.

(a) Asymmetric undoped $Al_xGa_{1-x}As/GaAs$ ($x = 0.1-0.25$) structures with three quantum wells separated by thin transparent barrier layers; such a structure represents a single two-dimensional electron system with a width of about 250–350 Å and with several levels of size quantization. A layer-by-layer arrangement of one such heterostructure (S1) is illustrated in Table 1 and its energy profile, levels of size quantization, and appropriate electron wave functions are shown in Fig. 4a.

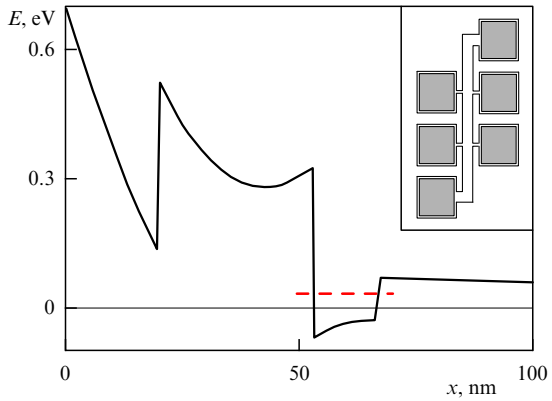

Figure 5. Energy profile of an asymmetric doped S512 heterostructure of $Al_xGa_{1-x}As/In_xGa_{1-x}As/GaAs$ system with a single level of size quantization (dashed line). In the inset to the figure is shown a planar form of the heterostructure samples prepared using lithography, with metallized bonding pads (for explanations, see the main text).

Table 2. Structure of an asymmetric doped heterostructure (S512) representing a single quantum well located between two barriers significantly differing in height (see Fig. 5).

Layer composition	Layer thickness, Å	x	Silicon concentration	Comment
GaAs	200		3×10^{17} cm^{-3}	Protective layer
$Al_xGa_{1-x}As$	300	0.28	7×10^{17} cm^{-3}	Doped region
$Al_xGa_{1-x}As$	30	0.28		Spacer
$In_xGa_{1-x}As$	135	0.2		Quantum well
GaAs	4300			Buffer layer

(b) Asymmetric undoped $Al_xGa_{1-x}As/GaAs$ ($x = 0.1-0.25$) structures with three quantum wells separated by thick barriers that are impenetrable to electrons, so that the three two-dimensional electronic layers are independent of each other (see data for the structure S1a in Table 1 and in Fig. 4b).

(c) Asymmetric doped heterostructure (S512) which represents a single quantum well $In_xGa_{1-x}As$ ($x = 0.2$) with a width of 135 Å between barriers of $Al_xGa_{1-x}As$ ($x = 0.28$) and GaAs that differ significantly in height. The layer-by-layer arrangement of this heterostructure is given in Table 2 and its energy profile is displayed in Fig. 5. In this quantum well, there is one level of size quantization below the Fermi level. Due to silicon doping of the region of the outer barrier lying behind the spacer, equilibrium charge carriers exist in the system, whose two-dimensional density at room temperature is 1.2×10^{12} cm^{-2} (0.78×10^{12} cm^{-2} at $T = 4.2$ K).

Samples of the undoped S1 and S1a heterostructures rectangular in shape (with dimensions of approximately 8×2 mm) each had two alloyed metallic (indium) potential contacts symmetrically located opposite each other at a distance of several millimeters (Figs 6c and 6d). The samples of the doped structure S512, which were prepared with the aid of lithography, had a so-called spider form (see inset to Fig. 5) intended for the measurement of transport properties, and in the plan view they represented a narrow strip 57 μm wide, on which metallized regions of potential contacts that were connected by even narrower (10 μm) bridges located at a distance of 0.27 mm from each other were applied. The

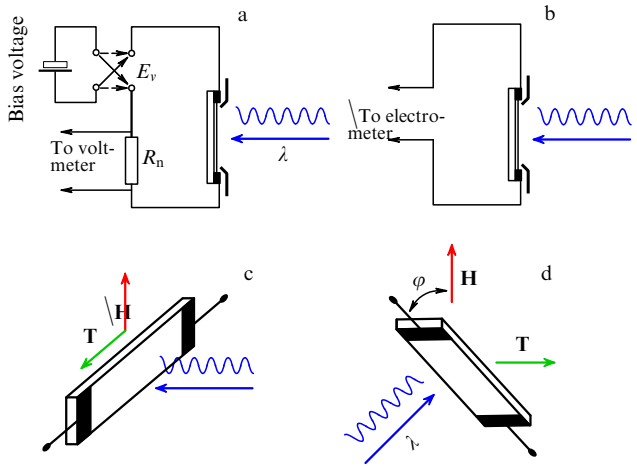

Figure 6. Geometry of experiments as well as the scheme of measurements of PGE and the longitudinal MEE (a, c), and the transverse MEE (b, d). Mutual orientations of the directions of the magnetic field and toroid moment relative to the plane of the heterostructure are shown.

overall length of the sample together with the bonding pads was 1.1 mm.

Measurements of the PGE and MEE were conducted in a special insert with an optical lead-in, placed vertically into a Dewar-vessel insert in a superconducting solenoid for measurements at intermediate temperatures. Light from a halogen lamp or a blue light emitting diode was put into the sample via a flexible light guide. The power of the supplied radiation was 5 mW at most; the radiation power density on the illuminated surface of the sample was approximately 0.35 mW mm^{-2}. The contacts and the adjacent regions of the sample were shut with a special protective shield. When measuring the PGE and the longitudinal MEE, the planes of the sample heterostructure layers were oriented along the magnetic field in such a manner that the line of the potential contacts of the samples was perpendicular to the field direction (Fig. 6c). In the measurements of the transverse MEE, the line of the potential contacts of the samples was oriented at an angle to the direction of the magnetic field in such a manner that the line of contacts, the asymmetry vector of the structure, and the magnetic field vector were located in one plane (Fig. 6d).

The electric circuit for measuring the PGE and the MEE was quite simple. Electric polarization in the magnetoelectric effect was measured on the potential contacts by a voltmeter with a very high input resistance or by an electrometer (Fig. 6b). As far as the PGE is concerned, initially the PGE current was measured in a simple closed series circuit consisting of the sample and a standard measuring resistance (Fig. 6a) [44]. In this case, the current determined from the voltage drop across the measuring resistance is the short-circuit current, since the resistance of the samples even under maximum illumination is considerably greater than the measuring resistance. It was possible, if necessary, to include an additional source of voltage in the metering circuit. Under these conditions, for example, we studied the magnetoresistance of an asymmetric heterostructure in the case of photoinduced charge carriers [45] and measured the current–voltage characteristics of the samples [44]. Notice that the alloying of a metallic (in our case, indium) contact to a certain depth is accompanied by the appearance of a potential barrier near the quantum well, which results in the appearance of a region depleted of charge carriers under the contact and in its immediate vicinity. This depleted near-contact region has a very high resistance, especially at low temperatures. Furthermore, at low temperatures the current–voltage characteristic of the contact/heterostructure/contact system becomes strongly nonlinear owing to the nonlinear properties of the near-contact regions, which considerably distorts the measured field dependences $J_{\rm PGE}(H)$ [44]. Therefore, we further measured the PGE, just as the MEE, almost always in a broken circuit from the potential difference $U_{\rm PGE}$ across the contacts to the heterostructure with the aid of an electrometer or a voltmeter with a very high input resistance. In this case, the effect of near-contact regions was eliminated completely and, if necessary, the photogalvanic current $J_{\rm PGE}$ was determined from the measured potential drop $U_{\rm PGE}$ and the known magnitude of the electrical resistance of the heterostructure at a given level of light excitation of charge carriers.

Photogalvanic effect in a strong magnetic field. The first experimental evidence for the existence of a sufficiently strong PGE in asymmetric heterostructures corresponding to the theoretical predictions of Ref. [43] can be considered to be the work by Aleshchenko et al. [46]. The authors of Ref. [46] detected a shift in the current–voltage curves of a three-well asymmetric $Al_xGa_{1-x}As/GaAs$ ($x = 0.25$) heterostructure depending on the direction of a DC 5-kOe magnetic field by a certain magnitude (varying with temperature) $V_{\rm PGE}$ (~ 0.25 V at $T \approx 300$ K), which was called by the authors the PGE emf. It was understandable that it was of interest to investigate the PGE in detail in a wide range of magnetic fields and temperatures using heterostructures with various asymmetric profiles, and this was performed in our subsequent work, beginning with Ref. [44].

Figure 7 displays the results of measurements of the field dependences of the potential difference, $U_{\rm PGE}(H)$, on various samples of undoped three-well $Al_xGa_{1-x}As/GaAs$ ($x = 0.25$) heterostructures in magnetic fields of up to 140 kOe at various temperatures and intensities of illumination with a halogen lamp. It is seen from the data given in Figs 7a and 7b for the heterostructure S1 that in all the cases the $U_{\rm PGE}(H)$ dependences represent H-odd functions that are linear in weak fields and are nonmonotonic (with well pronounced extrema) in strong fields. Worthy of mention are the large values of $U_{\rm PGE}$, which reach at the maximum (at $H \approx 20$ kOe), depending on the temperature and illumination conditions, 2–8 V per cm of length of the illuminated region of the heterostructure. At room temperature, with allowance for the measured electrical resistance (≈ 150 MΩ), this corresponds to a photogalvanic current $J_{\rm PGE}^{\rm max} \approx 10$ nA, which coincides with the data obtained in the short-circuit regime [44].

A linear increase in $U_{\rm PGE}$ at small H is a direct consequence of relations (9) and (10), i.e., of the fact that the magnitude of the toroid moment is linear in H in weak magnetic fields. With an increase in the magnetic field, $U_{\rm PGE}$ passes through a maximum and then decreases noticeably. It is understandable from general considerations that, as the magnetic length $L_H = (\hbar c/eH)^{1/2}$ becomes, with increasing H, less than the dimension of the three-well quantum region of the heterostructure along the asymmetry vector, processes of magnetic localization begin to manifest themselves; as a result, the shape of the potential that holds the carriers affects their behavior to a much less extent. Thus, the magnitude of

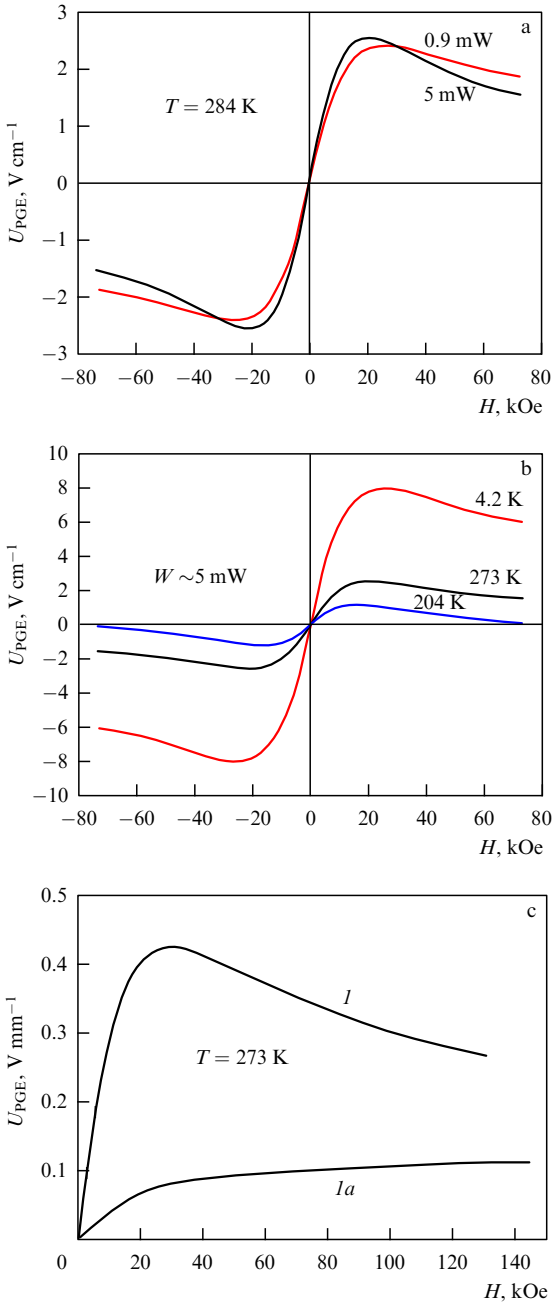

Figure 7. Field dependences $U_{PGE}(H)$ of the photogalvanic effect obtained on samples of asymmetric three-well undoped $Al_xGa_{1-x}As/GaAs$ ($x = 0.25$) heterostructures: (a) for the structure S1 at room temperature and illumination powers $W = 5$ and 0.9 mW; (b) for the structure S1 at $W = 5$ mW and $T = 273$, 204, and 4.2 K, and (c) for heterostructures with different tunnel coupling (curves *1* and *1a* refer to the structures S1 and S1a, respectively; see Table 1). The values of U_{PGE} are given in volts per unit length of the illuminated section of the heterostructure.

the asymmetry vector in formula (10) decreases in the range of strong fields with an increase in strength, and the toroid moment decreases correspondingly. The results of numerical calculations performed for the three-well heterostructure S1 in Ref. [45] show that with increasing H the electrons almost completely leave the two narrow quantum wells and are localized in the widest well. This leads not only to a strong decrease in the magnitude of the toroid moment, but also quite substantially affects the magnitude of the magnetoresistance when the photoinduced carriers are moving in the lateral plane of the heterostructure [$\Delta R(H)/R(0) = 1.85$ in a field of 75 kOe) [45], which in turn leads to a stronger field dependence of the photogalvanic current $J_{PGE}(H)$ as compared with $U_{PGE}(H)$ [44].

A comparison of the experimental data on the PGE, obtained in heterostructures with tunnel-coupled (S1) and separated (S1a) quantum wells gives evidence that the effect is much weaker in the samples with separated quantum wells (cf. curves *1* and *1a* in Fig. 7c) and in the field dependences of the PGE there is no maximum. The observed strong decrease in the PGE in the structures with narrow quantum wells separated by wide barrier layers impenetrable to electrons can be explained by the fact that in this case the toroidal states of the carriers are formed independently of each other in each quantum well whose potential energy profile and corresponding electron wave functions are much less asymmetric (Fig. 4b). As a consequence, the integral magnitude of the toroid moment induced by the magnetic field in each quantum well and in the entire structure on the whole proves to be considerably less than the one that could exist in the case of tunnel coupling between the quantum wells composing the structure. It is also understandable that the magnetic localization in this case must show itself only in very strong fields ($\sim$ 500 kOe), which explains the absence of a maximum in the PGE field dependences.

Transverse magnetoelectric effect in the undoped heterostructures of the AlGaAs/GaAs system. The results of measurements of the field dependences of electric polarization in circumstances where a transverse magnetoelectric effect occurs in samples of undoped three-well $Al_xGa_{1-x}As/GaAs$ ($x = 0.25$) heterostructures are presented in Fig. 8. All the data relate to the angle of inclination $\varphi = 45°$ of the heterostructure relative to the direction of the magnetic field, at which, according to formula (13), the effect is at a maximum. It is seen that in all the cases the $P_z(H)$ dependence take the form of symmetrical functions even in H. In the region of weak fields, where the toroid moment grows linearly with increasing field strength, the electric polarization is quadratic in the field, $P_z \sim H^2$. In contrast to the PGE, in which case the U_{PGE} passes through a maximum with an increase in H, the polarization in the transverse MEE continues growing in strong fields with a tendency to saturation, which is a consequence of two factors: a decrease, with increasing field strength, in the toroid moment induced by the lateral component H_z of the field [see formulas (11) and (13)], and a linear growth of the normal component H_x of the field. A comparison of the data on the transverse MEE, measured in heterostructures with tunnel-coupled and separated quantum wells, gives the same picture as that observed in the case of the PGE, namely, in samples with separated quantum wells the effect is considerably less delineated (cf. curves *1* and *1a* in Fig. 8c). The measurements of the transverse MEE, performed at different angles of inclination of the heterostructure plane to the direction of the magnetic field (Fig. 8d), showed that the angular dependence of the polarization follows expression (13) with a good accuracy.

Photogalvanic effect and transverse magnetoelectric effect in the doped heterostructure of the AlGaAs/InGaAs/GaAs system. Figure 9a displays the results of measurements of the field dependences $U_{PGE}(H)$ at room temperature in

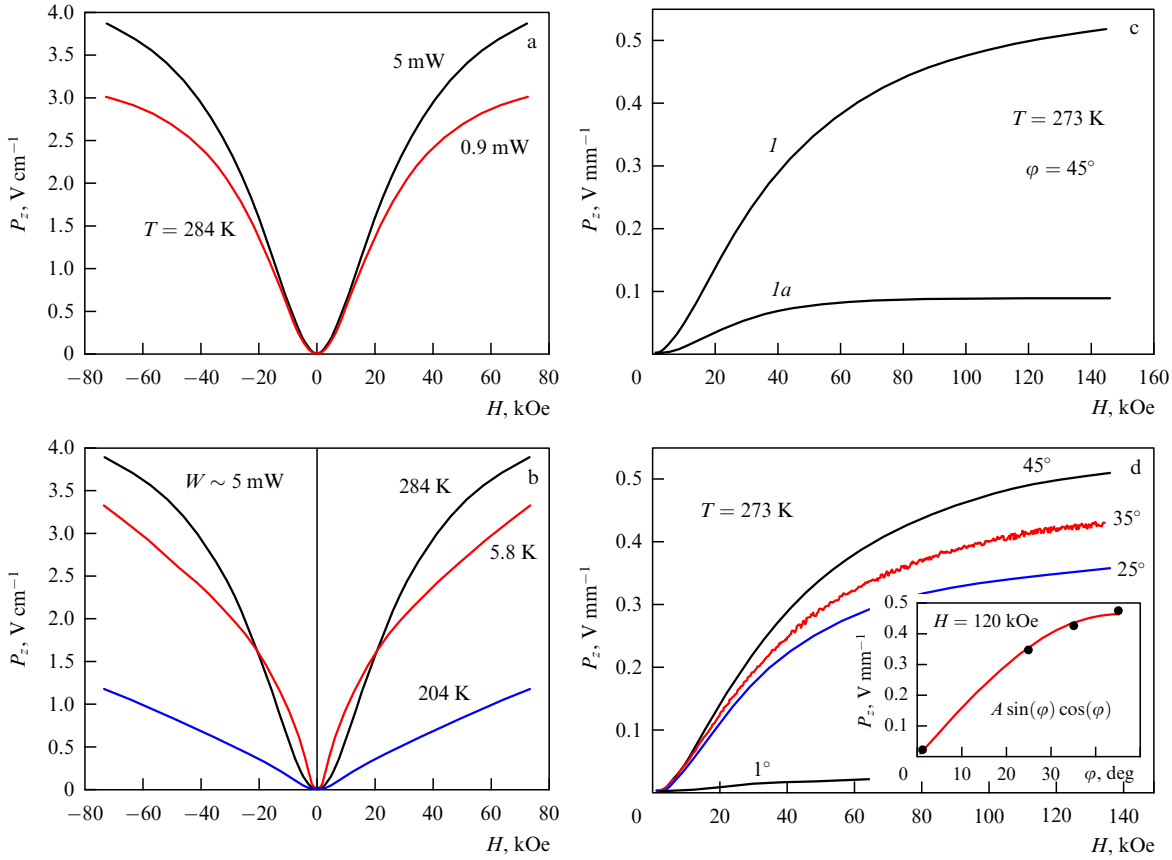

Figure 8. Field dependences of electric polarization $P_z(H)$ in the case of occurrence of the transverse magnetoelectric effect in samples of asymmetric three-well undoped $Al_xGa_{1-x}As/GaAs$ ($x = 0.25$) heterostructures: (a) for the S1 structure at room temperature and illumination powers $W = 5$ and 0.9 mW; (b) for the S1 structure at $W = 5$ mW and $T = 273$, 204, and 4.2 K; (c) for heterostructures with different tunnel coupling (curves *1* and *1a* refer to the structures S1 and S1a, respectively; see Table 1), and (d) at different inclinations of the heterostructure (S1) to the direction of the magnetic field (in the inset to the figure, the angular dependence of P_z at $H = 120$ kOe is given). The values of P_z are given in volts per unit length of the illuminated section of the heterostructure.

magnetic fields of up to 75 kOe in a sample of the doped heterostructure S512; shown in Fig. 9b are the results of measurements of the $P_z(H)$ dependences in the conditions of occurrence of the transverse magnetoelectric effect (the angle of inclination of the heterostructure with respect to the direction of the magnetic field is $\alpha = 45°$) in magnetic fields up to 140 kOe at room temperature (curve *1*) and at the liquid-helium temperature (curve *2*).

The measurements were made on adjacent potential contacts located at a distance of 0.27 mm from each other. The illumination was accomplished with a halogen lamp, which ensured, at a radiation power supplied to the sample on the order of 5 mW, a power density on the surface of the sample equal to 0.35 mW mm^{-2}. It follows from the comparison of the magnitudes of U_{PGE} at the maximum of the $U_{PGE}(H)$ dependence and of the electric polarization P_z in the region of its saturation in strong magnetic fields with the corresponding values for the undoped S1 heterostructure that at room temperature under equal illumination conditions the values of U_{PGE} and P_z reduced to a unit length of the illuminated section of the sample for the doped structure are less by a factor of approximately 3000.

The magnetoelectric effect in the doped structure, in contrast to that in the undoped structure, strongly depends on temperature: as the temperature decreases from room temperature to 4.2 K, P_z in the doped structure decreases by approximately an order of magnitude (see curve *2* in Fig. 9b). In this case, as can be seen from the data given, in the region of strong magnetic fields noticeably pronounced oscillations of $P_z(H)$ are observed. The period of these oscillations in the inverse magnetic field strength coincides with the period of oscillations for the Shubnikov–de Haas effect when measuring the field dependences of magnetoresistance in the case where the magnetic field is directed along the normal to the surface of the sample.

Both these facts, i.e., the strong weakening of the magnetoelectric effect with decreasing temperature and the presence of oscillations in the $P_z(H)$ dependence at low temperatures, indicate the above-mentioned participation of equilibrium carriers in the compensation for the electric polarization that arises due to the nonequilibrium photoinduced fraction of charge carriers. It is understandable that the extent of this compensation must be determined by the relaxation time τ in electron transport and, correspondingly, by the conductivity of the system ($\tau \ll \tau_r$, where τ_r is the recombination time of the photoinduced carriers). As the temperature decreases from room temperature to 4.2 K, the relaxation time τ increases substantially, which leads to an even larger compensation (in comparison with that observed at room temperature) for the electric dipole moment induced by the magnetic field, which, in addition, in strong magnetic fields ($\omega_c\tau \gg 1$, where ω_c is the cyclotron frequency) begins oscillating with the magnetic field.

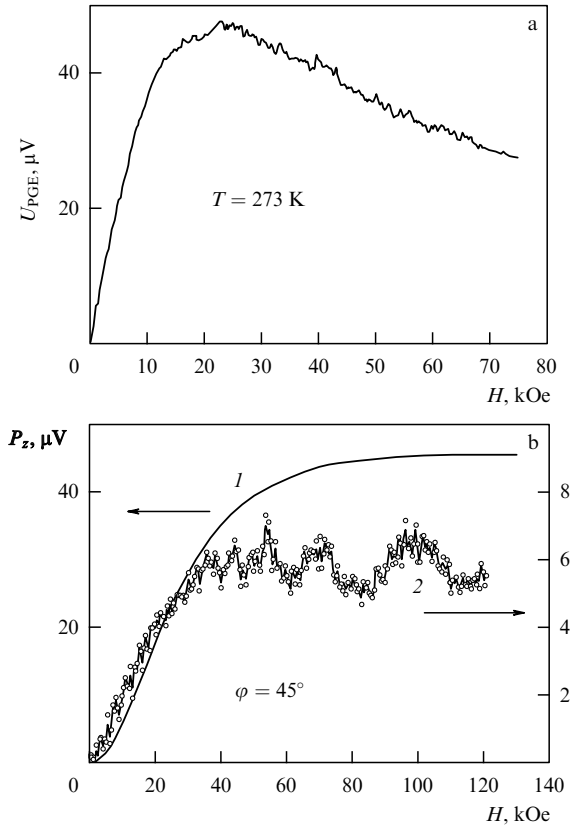

Figure 9. Field dependences of the photogalvanic effect: at $T = 273$ K (a), and electric polarization P_z in the transverse magnetoelectric effect (b) at $T = 273$ K (curve *1*) and 4.2 K (curve *2*) for a sample of an asymmetric doped S512 heterostructure.

3. At present, diverse manifestations of a new type of ordering are being experimentally discovered in condensed systems, namely, of toroidal ordering which was predicted at the beginning of the 1980s. A significant role in this discovery has been played by the methods of engineering the energy-band structure, which made it possible to observe the specific features of anomalous photogalvanic and magnetoelectric effects described in this report under nonequilibrium conditions in artificially grown heterostructures. Of large interest is the study of the possibility of existing a superdiamagnetic state in spatially inhomogeneous toroics, which is connected with the concept of a pseudomagnetic field [16] acting on the charge carriers.

It should be also noted that the magnetic field can break the symmetry of intrasubband transitions and lead to the occurrence of an APGE connected with the appearance of an additive, asymmetric in momentum, to the distribution function, which apparently was observed in work [47]. It is significant that the symmetry of the experiment in this case also allows the existence in the system of a toroid moment and allied asymmetry of the spectrum with respect to the quasimomentum, which can be responsible for the APGE examined in this report. A comparison and the revealing of differences in the experimental manifestations of the two mechanisms of the APGE — caused by the asymmetry of the distribution function in momentum in the symmetric in the electric field approximation [40, 47] and caused by the asymmetry of the spectrum [see Eqns (7)–(9)] — require additional study.

References

1. Gorbatsevich A A, Kapaev V V, Kopaev Yu V *Ferroelectrics* **161** 303 (1994)
2. Gorbatsevich A A, Kopaev Yu V *Ferroelectrics* **161** 321 (1994)
3. Landau L D, Lifshitz E M *Statisticheskaya Fizika* (Statistical Physics) Pt. 1 (Moscow: Nauka, 1976) p. 489 [Translated into English (Oxford: Pergamon Press, 1980)]
4. Ascher E, in *Magnetoelectric Interaction Phenomena in Crystals* (Eds A J Freeman, H Schmid) (New York: Gordon and Breach Sci. Publ., 1975) p. 69
5. Volkov B A, Gorbatsevich A A, Kopaev Yu V *Zh. Eksp. Teor. Fiz.* **86** 1870 (1984) [*Sov. Phys. JETP* **59** 1087 (1984)]
6. Smolenskii G A, Chupis I E *Usp. Fiz. Nauk* **137** 415 (1982) [*Sov. Phys. Usp.* **25** 475 (1982)]
7. Schmid H *Ferroelectrics* **162** 317 (1994)
8. Kimura T et al. *Nature* **426** 55 (2003)
9. Hur N et al. *Nature* **429** 392 (2004)
10. Eerenstein W, Mathur N D, Scott J F *Nature* **442** 759 (2006)
11. Ginzburg V L, Gorbatsevich A A, Kopaev Yu V, Volkov B A *Solid State Commun.* **50** 339 (1984)
12. Zel'dovich Ya B *Zh. Eksp. Teor. Fiz.* **33** 1531 (1957) [*Sov. Phys. JETP* **6** 1184 (1958)]
13. Ascher E *Helv. Phys. Acta* **39** 40 (1966)
14. Ascher E *Int. J. Magn.* **5** 287 (1974)
15. Landau L D (unpublished)
16. Gorbatsevich A A *Zh. Eksp. Teor. Fiz.* **95** 1467 (1989) [*Sov. Phys. JETP* **68** 847 (1989)]
17. Dubovik V M, Cheshkov A A *Fiz. Elem. Chastits At. Yadra* **5** 791 (1974) [*Sov. J. Part. Nucl.* **5** 318 (1974)]
18. Dubovik V M, Tosunyan L A *Fiz. Elem. Chastits At. Yadra* **14** 1193 (1983) [*Sov. J. Part. Nucl.* **14** 504 (1983)]
19. Landau L D, Lifshitz E M *Teoriya Polya* (The Classical Theory of Fields) (Moscow: Nauka, 1988) p. 136 [Translated into English (Oxford: Pergamon Press, 1983)]
20. Spaldin N A, Fiebig M, Mostovoy M *J. Phys. Condens. Matter* **20** 434203 (2008)
21. Dubovik V M, Krotov S S, Tugushev V V *Kristallografiya* **32** 540 (1987) [*Sov. Phys. Crystallogr.* **32** 314 (1987)]
22. Dubovik V M, Tugushev V V *Phys. Rep.* **187** 145 (1990)
23. Sannikov D G *Pis'ma Zh. Eksp. Teor. Fiz.* **41** 229 (1985) [*JETP Lett.* **41** 277 (1985)]
24. Sannikov D G, Zheludev I S *Fiz. Tverd. Tela* **27** 1369 (1985) [*Sov. Phys. Solid State* **27** 826 (1985)]
25. Ederer C, Spaldin N A *Phys. Rev. B* **76** 214404 (2007)
26. Popov Yu F et al. *Pis'ma Zh. Eksp. Teor. Fiz.* **69** 302 (1999) [*JETP Lett.* **69** 330 (1999)]
27. Popov Yu F et al. *Zh. Eksp. Teor. Fiz.* **114** 263 (1998) [*JETP* **87** 146 (1998)]
28. Van Aken B B et al. *Nature* **449** 702 (2007)
29. Affleck I, Marston J B *Phys. Rev. B* **37** 3774 (1988)
30. Shoenberg D *Magnetic Oscillations in Metals* (Cambridge: Cambridge Univ. Press, 1984) [Translated into Russian (Moscow: Mir, 1986)]
31. Privorotskii I A *Zh. Eksp. Teor. Fiz.* **52** 1755 (1967) [*Sov. Phys. JETP* **25** 1167 (1967)]
32. Girvin S M, MacDonald A H *Phys. Rev. Lett.* **58** 1252 (1987)
33. Zhang S C, Hansson T H, Kivelson S *Phys. Rev. Lett.* **62** 82 (1989)
34. Volovik G E *The Universe in a Helium Droplet* (New York: Oxford Univ. Press, 2003)
35. Kalmeyer V, Laughlin R B *Phys. Rev. Lett.* **59** 2095 (1987)
36. Halperin B I, March-Russell J, Wilczek F *Phys. Rev. B* **40** 8726 (1989)
37. Sawada K, Nagaosa N *Phys. Rev. Lett.* **95** 237402 (2005)
38. Jung J H et al. *Phys. Rev. Lett.* **93** 037403 (2004)
39. Belinicher V I, Sturman B I *Usp. Fiz. Nauk* **130** 415 (1980) [*Sov. Phys. Usp.* **23** 199 (1980)]
40. Ivchenko E L, Pikus G E, in *Problemy Sovremennoi Fiziki: Sbornik Statei k 100-letiyu so Dnya Rozhdeniya A.F. Ioffe* (Problems of Modern Physics: Collected Papers on the Occasion of Centenary of the Birth of A.F. Ioffe) (Exec. Ed. A P Aleksandrov) (Leningrad: Nauka, 1980) p. 275

41. Ivchenko E L, Pikus G E *Superlattices and Other Heterostructures: Symmetry and Optical Phenomena* (Springer Series in Solid-State Sciences, Vol. 110) 2nd ed. (Berlin: Springer, 1997)
42. Sturman B I, Fridkin V M *Fotogal'vanicheskii Effekt v Sredakh bez Tsentra Simmetrii i Rodstvennye Yavleniya* (Photogalvanic Effect in Media without a Center of Symmetry and the Related Phenomena) (Moscow: Nauka, 1992)
43. Gorbatsevich A A, Kapaev V V, Kopaev Yu V *Pis'ma Zh. Eksp. Teor. Fiz.* **57** 565 (1993) [*JETP Lett.* **57** 580 (1993)]
44. Omel'yanovskii O E, Tsebro V I, Kadushkin V I *Pis'ma Zh. Eksp. Teor. Fiz.* **63** 197 (1996) [*JETP Lett.* **63** 209 (1996)]
45. Tsebro V I et al. *Phys. Low-Dim. Struct.* (1/2) 25 (1997)
46. Aleshchenko Yu A et al. *Pis'ma Zh. Eksp. Teor. Fiz.* **58** 377 (1993) [*JETP Lett.* **58** 384 (1993)]
47. Emelyanov S A, Meltser B Ya, Ivanov S V *Pis'ma Zh. Eksp. Teor. Fiz.* **76** 547 (2002) [*JETP Lett.* **76** 469 (2002)]

PACS numbers: **75.80.+q**, **77.80.–e**
DOI: 10.3367/UFNe.0179.200908i.0897

Inhomogeneous magnetoelectric interaction in multiferroics and related new physical effects

A K Zvezdin, A P Pyatakov

1. Introduction

In this report, we consider a variety of phenomena related to inhomogeneous magnetoelectric interaction. The interconnection between the spatial modulation of the order parameter and electric polarization, known as the flexoelectric effect in liquid crystals, in the case of multiferroics manifests itself in the form of spin modulation induced by electric polarization, and as an inverse effect of formation of spin-induced electric polarization. This *flexomagnetoelectric* interaction also underlies the influence of the ferroelectric domain structure on the antiferromagnetic structure and the magnetoelectric properties of micromagnetic structures. We also consider the influence of an inhomogeneous magnetoelectric effect on the dynamic properties of multiferroics, in particular, on the magnon spectra.

The last decade has been characterized by a spate of interest in media with interrelated magnetic and electrical properties* (see reviews [1–10], and also special issues of two journals devoted to this problem [11]). The interest in this area is expressed, on the one hand, by enhanced attention paid to the fundamental aspects of magnetoelectric phenomena in multiferroics (substances in which magnetic and electric orderings coexist), and, on the other hand, by the expectation of concrete practical applications of magnetoelectrics in spin electronics (in particular, as the base for magnetic-memory devices) and in sensor technology.

The application of multiferroics will make it possible to significantly enlarge the functional possibilities of spintronics: a new degree of freedom — electric polarization — provides the additional means to tune the magnetic and magnetoresistive properties of spintronic elements [12] and to realize four-state logical units [13, 14]. Moreover, the use of magnetoelectric phenomena will make it possible in perspective to avoid using electric currents for magnetic recording [15–18], which is quite timely, since the progressively developing miniaturization of the traditionally used inductive elements is encountering the problem of excessive heat release because of an increase in the current density [19].

An enhanced interest in the fundamental mechanisms of interaction between magnetic and electric subsystems in solids has also been observed lately [10, 20–27], and the variety of types of magnetoelectric interactions has grown noticeably. In the classical review [28], which reflected the level of knowledge on multiferroics in the early 1980s, it was assumed that the polarization $\mathbf{P}$ and the magnetizations $\mathbf{M}_s$ of the sublattices (here s is the order number of a magnetic sublattice) were coupled mainly via the interaction of the form

$$F^{\mathrm{ME}} = -\frac{1}{2}\sum_{ss'} \gamma_{ss'}^{ijkl} P^i P^j M_s^k M_{s'}^l ,$$

which did not require any additional conditions except for the very existence of magnetic and electric ordering; recently, however, other interaction modes, introduced in Ref. [28], have come to the foreground, namely, those that are linear in the order parameters. In particular, the association of electric polarization with the presence of spatially modulated spin structures in the substance was established [29–31], and effects odd with respect to field, which make it possible to control the magnetic structure with the aid of an electric field, have also been discovered [32–35]. Whatever the origin of spatial modulation, i.e., whether as a result of competing exchange interactions, as in frustrated multiferroics [29–33], as a result of the magnetoelectric nature, as in bismuth ferrite [1, 36], or as a result of establishing equilibrium micromagnetic configuration [34, 35], in all cases nonzero spatial derivatives of the magnetic order parameter, $\nabla_i M_j$, existed, which created prerequisites for the manifestation of inhomogeneous *magnetoelectric interaction*.

2. Inhomogeneous magnetoelectric (flexomagnetoelectric) interaction

The inhomogeneous magnetoelectric interaction of the $P_i n_j \nabla_k n_l$ type, where $\mathbf{n}$ is the unit vector of the magnetic order parameter (magnetization or the antiferromagnetic vector), was introduced in Refs [37, 38] in connection with the possibility of the appearance, in magnetically ordered crystals, of long-period structures, and with the possibility of the manifestation of the inverse effect of the formation of electric polarization at domain boundaries [39]. The close analogy between the spatially modulated spin structures in ferroelectromagnets and the spatial modulation of the director in nematic liquid crystals has been noted in Ref. [40]: it manifests itself in the similarity of the mathematical expressions for the energy of inhomogeneous magnetoelectric interaction in ferroelectromagnets and the energy of flexoelectric interaction in liquid crystals, where the director $\mathbf{n}$ serves as the order parameter. This gives grounds to call the inhomogeneous magnetoelectric interaction the *flexomagnetoelectric* interaction.

In the isotropic case or in the case of cubic symmetry, the inhomogeneous magnetoelectric interaction, to an accuracy of the total derivative, takes on an elegant form [40]

$$F_{\mathrm{flexo}} = \gamma \mathbf{P}\big(\mathbf{n}\,\mathrm{div}\,\mathbf{n} + [\mathbf{n}\times \mathrm{rot}\,\mathbf{n}]\big) . \qquad (1)$$

* Since the mid-1990s, the number of published works devoted to magnetoelectric materials has increased twofold–threefold every five years, and has reached about 800 publications per year.